Spin-wave resonance in high-conductivity films: The Fe-Co alloy system

F. Schreiber*
Institut für Experimentalphysik III, Ruhr-Universität Bochum, 44780 Bochum, Germany

Z. Frait
Institute of Physics, Academy of Sciences of the Czech Republic, 18040 Prague 8, Czech Republic
(Received 8 December 1995; revised manuscript received 11 April 1996)

A detailed standing spin-wave resonance (SSWR) study in the frequency range 17–69 GHz in normal and parallel configurations is presented for Fe_xCo_{1-x} alloy films. The implications of the use of different approximate theoretical descriptions for the line positions, widths, and intensities are investigated and compared to the complete theory which includes the coupling of the spin waves to electromagnetic waves by means of the high conductivity of the material. For $x=0.55$, the exchange parameter A is determined to be 2.7×10^{-6} erg/cm, i.e., significantly higher than for pure Fe (2.0×10^{-6} erg/cm). In contrast, the g factor and the damping constant λ are almost the same for $x=0.55$ and 1. The problem of interpretation of the surface anisotropy parameter K_s obtained by different experimental methods on different film thicknesses is discussed. [S0163-1829(96)05730-X]

I. INTRODUCTION

Because of the wealth of information accessible, standing spin-wave resonance (SSWR) and ferromagnetic resonance (FMR) belong to the classical experimental methods in the field of magnetism.[1–4] The spectra depend on the magnetization, surface and volume anisotropies, direct and indirect exchange interactions, the g factor, damping, conductivity, etc., which, on the other hand, also require an elaborate analysis in many cases.

Various approximations have been used for the theoretical description,[2] and effects related to the finite electrical resistivity ρ of a metal are often neglected. The latter complicate the theory considerably, and, e.g., the quite complex case of the external field parallel to the film plane [parallel configuration (PC)] was only recently treated in detail with introducing formulae for the surface impedance Z.[5] Generally, much work was devoted to the understanding of SSWR spectra but, remarkably, despite the precision achievable by the method, the potential was not fully exploited for the extraction of information on various magnetic materials, and most of the work was done only on certain systems, mainly on Permalloy ($Fe_{20}Ni_{80}$).

In a recent short note,[6] Fe_xCo_{1-x} was found to show a remarkable concentration dependence of the Landau-Lifshitz damping parameter λ and the g factor g, with both quantities exhibiting a plateau for x larger than $\sim$ 0.5 and an increase on the Co-rich side. It could be shown that the investigation of the mutual relationship between $g(x)$ and $\lambda(x)$ helps to understand the relevant interaction, i.e., the spin-orbit coupling in this case.[6,7] The system Fe_xCo_{1-x} is also suitable for first principles electronic structure calculations,[8] and a comparison with experimental data is challenging.

The aim of the present paper is twofold. First, we determine the physical quantities of Fe_xCo_{1-x} films accessible by SSWR which, to our knowledge, has not been done before and which should contribute to a more complete picture of this alloy system. We focus on $x\approx0.55$ where the Curie temperature $T_C(x)$ has its maximum (1243 K) for the bcc phase,[9] indicating a strong exchange interaction. This concentration is close to the limit of the above-mentioned plateau of $g(x)$ and $\lambda(x)$, and the magnetocrystalline anisotropy is low which often favors narrow resonance lines. Second, we analyze the implications of different theoretical approaches with emphasis on the modifications that occur when a relatively low ρ as that of Fe-Co is taken into account. Finally, we discuss some aspects that are relevant for the interpretation of the surface anisotropy K_s obtained by different methods.

In Sec. II, we explain the theoretical principles. Some experimental details are given in Sec. III. The results together with different steps of the analysis are presented in Sec. IV. Section V is devoted to the discussion of the results and their interpretation.

II. THEORY

The development of the theoretical description may be roughly separated into three steps which we sketch briefly (KT, IT, and CT stand for Kittel's, insulator, and complete theory, respectively; see below). The equation of motion for non-uniform excitations is

$$\frac{\partial\vec{M}}{\partial t}=\gamma\vec{M}\times\left[\vec{H}_i+\frac{2A}{M^2}\nabla^2\vec{M}-\frac{\lambda}{\gamma M^2}(\vec{M}\times\vec{H}_i)\right], \qquad (1)$$

where M denotes the magnetization, $\gamma=g\mu_B/\hbar$ the gyromagnetic ratio, and A the exchange parameter. The last term on the right-hand side describes the Landau-Lifshitz damping. The internal field H_i includes the interactions of M with the external static magnetic field H, dipolar fields, anisotropy fields, etc.[3,4]

In the most popular case of H and M perpendicular to the surface [normal configuration (NC)], the resonance condition in the simplest form is[2]

$$\left(\frac{\omega}{\gamma}\right)=H-4\pi M+\left(\frac{2A}{M}\right)k^2, \tag{2}$$

where $\omega/(2\pi)$ is the microwave frequency and k the wave number of the spin wave. In general, additional uniaxial anisotropies may be taken into account but these are small for our films.

The boundary conditions determine the possible k values. KT as the simplest approximation assumes ''perfect pinning'' of the spins at the surface, thus leading to $k=n\pi/d$, where n is an integer and d the thickness.

In a further step, an arbitrary value of pinning is introduced in the form of Néel's surface anisotropy

$$E_s=K_s\sin^2\Theta. \tag{3}$$

The possible k values are then determined from[2]

$$\cot(kd/2)=\frac{2A}{K_s}k, \qquad -\tan(kd/2)=\frac{2A}{K_s}k. \tag{4}$$

This model will be called IT. It reduces to KT for $K_s\to\infty$. As can be seen from Eqs. (4) or their graphical solution[2] the difference between IT and KT is most pronounced for the low modes. There also exists a solution with imaginary k (surface mode) in the NC for $K_s<0$ and in the PC for $K_s>0$. Many authors have discussed their results in terms of the above concept or its modifications, and various aspects have been highlighted.[2,10–12] Recently, Portis' idea of spin waves in films with a tailored magnetization profile $M=M(z)$ was experimentally investigated.[13]

However, the above approach is still the insulator approximation. Effects related to the finite penetration depth δ of the high-frequency field (skin effect) and to coupled electromagnetic and spin waves are neglected. If a finite ρ is taken into account (together with finite K_s and λ which we will refer to as CT), the theoretical description becomes significantly more complicated. We only indicate the main ingredients (for details, see, e.g., Refs. 2,5). Equation (1) together with Maxwell's equations

$$\nabla\times\vec{e}=-\frac{1}{c}\frac{\partial(\vec{h}+4\pi\vec{m})}{\partial t}, \qquad \nabla\times\vec{h}=\frac{4\pi\sigma}{c}\vec{e} \tag{5}$$

yields three relations for the components of the high-frequency magnetic field and magnetization, $\vec{h}$ and $\vec{m}$. $\vec{e}$ is the electrical field, σ the conductivity, and c the velocity of light. The resulting secular equation for the wave numbers is biquadratic for the NC and bicubic for the PC.[5] After applying appropriate boundary conditions[2,14] for $\vec{h}$ and $\vec{m}$, finally (following rather long algebra), the tangential components (e_t and h_t) of $\vec{e}$ and $\vec{h}$ are determined and, hence, the normalized surface impedance[2]

$$Z=\sqrt{2\pi A}\frac{2}{10^3\rho Mc}\left(\frac{e_t}{h_t}\right)_{\text{surface}}, \tag{6}$$

which depends on H, ω, γ, M, K_s, A, λ, ρ, and d in a nontrivial way.

Although the insulator approximation is quite often used as it is much more convenient to deal with, it is by no means clear *a priori* that this is justified, particularly in the case of a system with a relatively high conductivity such as Fe-Co. Pronounced changes may be expected if δ comes into the range of k. We stress that δ is reduced at resonance in comparison to the ''nonresonance'' (conventional skin-effect) case. E.g., for material parameters typical for Fe-Co, the calculations yield a reduction from $\sim10^{-4}$ cm to $\sim2\times10^{-6}$ cm (for $K_s=0$; for $K_s=+0.5$ erg/cm^2, we find $\sim3\times10^{-6}$ cm and $\sim4\times10^{-6}$ cm for $K_s=-0.5$ erg/cm^2) for the active wave (positively circularly polarized, Kittel mode[2]) in the NC at 23 GHz. In the PC, δ at resonance is $\sim3\times10^{-6}$ cm for each of the K_s values.

III. EXPERIMENT

The samples were prepared in an rf-sputter system described previously.[6,15] Two different types of substrates were used. On MgO(001), single-crystalline films of good quality were obtained but the single-crystalline growth could not be extended to $d\sim$ 1000 Å which would have been particularly useful for SSWR. Therefore, the series to which we mainly refer is polycrystalline and grown on glass (800–1900 Å). All Fe-Co films were covered with a 40 Å Au layer to prevent oxidation. Essentially the same characterization scheme was applied as described in Refs. 6,15 employing x-ray diffraction and scanning electron microscopy with energy-dispersive x-ray analysis. As an additional magnetic characterization tool, hysteresis loops were measured by microwave absorption, yielding low coercive forces (for some films $H_c<$ 10 G).

The SSWR spectra were measured in a shortened waveguide setup at 17, 23, 48, and 69 GHz with a maximum field of 31 kG. The sample could be placed at various positions in the magnetic and electric high-frequency fields (see different excitation conditions described in Sec. IV and Fig. 5). Both the microwave frequency and the static field could be measured with high precision (better than 10^{-6} and 10^{-4}, respectively; for sensitivity and accuracy, see also Refs. 16,17).

Measurements in a broad frequency range are useful for a number of reasons. In general, the accuracy of the determination of several quantities is increased, e.g., g factor, damping parameter, anisotropies, etc. Moreover, there are SSWR-specific advantages. In the NC, the field interval for spin waves is of the order of ω/γ (saturation field of the order of $4\pi M$, lowest-order mode at about $\omega/\gamma+4\pi M$). As the analysis is more precise the larger the interval and the more modes are observable, especially high frequencies, are useful. A similar argument holds for the PC where the low-field limit is not the saturation but simply the zero field. In addition, the possibility to measure at different values of the ellipticity in the PC is an important point (see Sec. IV), particularly if $4\pi M$ is high. In this respect, due to its high magnetization, Fe-Co is experimentally more difficult for SSWR than, e.g., Permalloy (which also has a higher resistivity, causing a less strong exchange-conductivity broadening).

IV. RESULTS AND ANALYSIS

In the following, we present the experimental data and explain their analysis. The resulting parameters displayed in

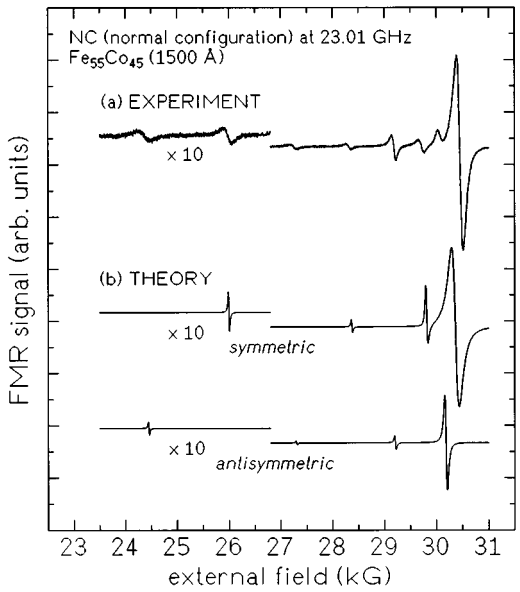

FIG. 1. (a) 23.01 GHz spectrum in the NC for a film on glass with $d=1500$ Å and $x=0.55$. (b) Theoretical spectrum calculated using $A=2.43\times10^{-6}$ erg/cm, $4\pi M=$ 22.55 kG, $K_s=0.5$ erg/cm^2, $g=2.09$, $\rho=8\times10^{-6}$ Ω cm, and $\lambda=6.5\times10^7$ rad/s. For clarity, the symmetric and the antisymmetric parts are indicated.

Table I are obtained from a simultaneous fit for all frequencies and orientations using the CT. For clarity, we separately discuss the NC and PC and try to indicate which observable is influenced most by which material parameter. The mode spacing, e.g., is certainly the main feature for the determination of A. It is also used for a first discussion of the approximate theories. We concentrate on the samples with d around 1200–1500 Å as they yield the most transparent results. For smaller d, fewer lines are observed, and for higher d, the intensity $I(n)$ decreases more rapidly which makes the analysis also more difficult.

A. Normal configuration (NC)

In Fig. 1, we show a typical NC spectrum at 23 GHz. The line positions H_n are displayed in Fig. 2. In a first step (KT), one may obtain an estimate for A from the slope of H_n versus n^2 (for higher-order modes), i.e., assuming infinite K_s. For our samples, the value for A would be of the order of 2×10^{-6} erg/cm. With this crude assumption the agreement is limited, and, particularly, the curvature of $H_n(n^2)$ for low n causes deviations.

TABLE I. Parameters for the simultaneous fits of the SSWR spectra at different frequencies in different orientations using the complete theory. We give here the values averaged over a series of samples representative for $Fe_{55}Co_{45}$. The main parameter of interest, A, scattered by about (5–10)%, mainly due to uncertainties in the determination of the thickness. ρ is $\sim$ 10% higher than the bulk value (Ref. 9) to fit $\Delta H(n=1)$ in the NC. For the surface anisotropy we obtained $K_s=$ 0.5 erg/cm^2.

$4\pi M$ (kG)	g	A (10^{-6} erg/cm)	ρ (10^{-6} Ω cm)	λ (10^7 rad/s)
22.7	2.09	2.7	8.0	6.5

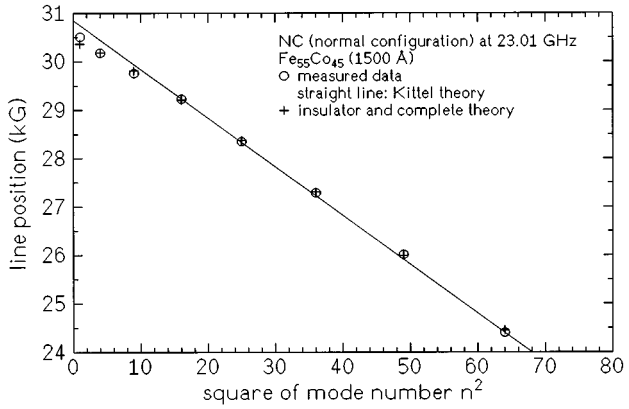

FIG. 2. Line positions H_n of Fig. 1 as a function of n^2. The slope of the straight line (KT) corresponds to $2A/M=2.4\times10^{-9}$ G cm^2. The fit using IT and CT yields $K_s=0.5$ erg/cm^2 and $2A/M=2.7\times10^{-9}$ G cm^2.

An improvement is achieved by taking into account a finite K_s. It is useful to look first at the expansion of the IT [Eqs. (4)] in the vincinity of the solutions for $2A/(K_sd)\to0$ (KT), i.e., around $kd=n\pi$. For $|2A/(K_sd)\ll1|$ and not too high n we obtain in lowest order

$$(kd)_{\mathrm{IT}}\approx n\pi\left(1-\frac{A}{K_sd}+\cdots-\cdots\right) \tag{7}$$

and, thus,

$$A_{\mathrm{IT}}\approx A_{\mathrm{KT}}\left(1+\frac{2A}{K_sd}+\cdots-\cdots\right). \tag{8}$$

So, for a *positive* K_s, the real A is *underestimated* by analyzing with the assumption of perfect pinning. The curvature of $H_n(n^2)$ is obtained in higher orders, and for $K_s>0$ the slope of $H(n^2)$ becomes smaller for low n which is the case here. It is also readily seen that for very high n the slope of $H(n^2)$ is independent of K_s but this situation is practically not reached for the present samples. The final fit displayed in Fig. 2 is obtained using IT/CT, and the parameters are given in the figure captions. It should be noted that for IT and CT n is not connected with k in the sense of KT but represents the mode number, i.e., the branch of the solution of Eqs. (4) for IT.

For this thickness (1500 Å) and the material parameters of Fe-Co, it is found that the difference between IT and CT concerning the line *positions* is very small. Our simulations yielded a shift of H_n by <2 G when changing ρ by several orders of magnitude. However, this applies only to $K_s>0$ found in our films (see also Sec. V). For negative K_s, the difference between IT and CT can be significant.[16]

Inhomogeneities in the films may cause deviations from a simple quadratic dependence of H_n on k as discussed, e.g., in Refs. 18,19. These are usually more pronounced for the low-order modes. Some authors discuss this in terms of the so-called ''Portis well'' defined by the comparison of the exchange energy of the modes with that associated with the internal field inhomogeneity.[19] For our samples, essentially only the main mode exhibits a deviation from the theoretical curve, and, consequently, all other modes are located out of

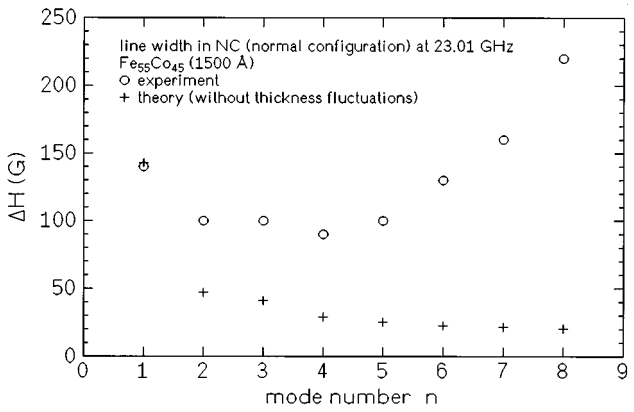

FIG. 3. Line width ΔH as a function of mode number n at 23.01 GHz in the NC for $d=$ 1500 Å . The deviation between theory and experiment for higher n is explained by a small lateral variation of the thickness (see text).

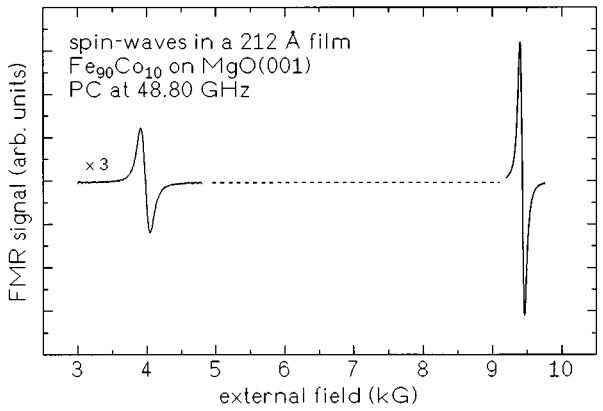

FIG. 4. 48.80 GHz spectrum of a 212 Å single-crystalline film on MgO(001) with $x=0.9$ in the PC. The external field is applied along the hard axis in the plane, i.e., the [110] axis of the film. The spacing between the main mode and the first low-field satellite is very high (5.46 kG) due to the small thickness. It is similar for the easy axis and corresponds to $2A/M=2.5\times10^{-9}$ G cm^2.

the Portis well [$(2A/M)k^2>\delta H_{\rm int}$]. The internal field inhomogeneity can be estimated using the value $H^*_{n=1}$ obtained by extrapolation from the high-order modes,

$$\delta(H_{\rm int})\approx H_{n=1}-H^*_{n=1}, \tag{9}$$

yielding some 0.01–0.1 kG for our films. 0.1 kG.

The experimental finding of a minimum of the linewidth, ΔH, for intermediate n as shown in Fig. 3 is common for the whole series. Due to the low ρ, the exchange-conductivity broadening[2] is quite strong for the main mode but this effect decreases rapidly with increasing n and the theoretical curve is then governed by the Landau-Lifshitz damping.

The deviation between theory and experiment for higher n which has also been found by other authors, e.g., for Permalloy films[20] may be explained by assuming a small lateral thickness fluctuation δd, which leads to a broadening proportional to n^2,

$$\left|\frac{\partial H}{\partial k}\frac{\partial k}{\partial d}\delta d\right|=\frac{2A}{M}\left(\frac{n\pi}{d}\right)^2\frac{2\,\delta d}{d}. \tag{10}$$

$\delta d/d$ is of the order of 1% for our films (assuming $k=n\pi/d$). Equation (10) is, however, only a simple picture. For a more sophisticated theoretical treatment of $\Delta H(n)$ (including dipolar and exchange coupling, but neglecting conductivity contributions) and its dependence on different kinds of fluctuations see, e.g., Ref. 21.

The effects of different intrinsic parameters on ΔH for the main mode are the following. As mentioned above, the exchange-conductivity broadening is dominating. As ΔH increases almost linearly with decreasing ρ, it is clear that the lines for Fe-Co are broader than for Permalloy ($\rho=14\times10^{-6}\ \Omega$ cm). For thicker films, this broadening source is more effective; e.g., for 1500 Å , ΔH is $\sim$ 30 G higher than for 1200 Å . In the range of $d\sim200$ Å , it can be neglected for most practical purposes (only $\sim$ 2 G).[22] An increase of A also leads to a broader line but this effect is relatively weak as well as the broadening with increasing K_s in the NC (in the PC, an increase of K_s narrows the line).

The intensity I, defined as the area under the absorption curve [second field integral of the measured derivative signal which is proportional to $S_p\times(\Delta H)^2$ where S_p is the peak signal], is expected to behave like $I\sim n^{-2}$ for perfect pinning (KT). For finite K_s, I falls off faster with n which is the case for the present films.

Our simulations using CT show that the conductivity significantly changes $I(n)$ as was also discussed in Ref. 11 for Permalloy. As this phenomenon is connected with a finite δ, the influence of ρ on $I(n)$ depends also on d and K_s. Due to the complexity of the problem, it is clear that $I(n)$ can only properly be described by CT. However, an accurate and reliable analysis of intensities is quite a complicated task as $I(n)$ can be strongly influenced by inhomogeneities within the film volume[19] which are difficult to incorporate in the CT (in Ref. 19, the insulator approximation was used together with limiting cases for K_s).

B. Parallel configuration

Measurements with the external field in the film plane are less popular in SSWR and their analysis is somewhat less direct. As indicated in Sec. II, the theory is more complicated, and usually a smaller number of modes can be observed, but, of course, a complete SSWR analysis has to reflect also on the PC spectra. accuracy. For SSWR investigations, particularly at various frequencies, the following points are important.

First, in some cases the PC may be even more useful than the NC for the detection of other than the main mode. When the mode spacing ($\sim d^{-2}$) for very thin films is so high that it is of the order of (or even exceeds) the disposable field interval in the NC ($\sim\omega/\gamma$, with ω low enough for the main mode still below the maximum field of the apparatus), PC measurements at higher frequencies are the only way because there the disposable field interval is higher, e.g., for 69 GHz, about 15 kG between the main mode and zero field. An example of this rarely applied ''technique'' is shown in Fig. 4 for a sample with $d=$ 212 Å belonging to our single-crystalline series grown on MgO(001).

Second, the ellipticity of the magnetization precession, the effective surface anisotropy $K_s^{\rm eff}$ (see Ref. 2), and the

intensity of higher-order modes can significantly change for different frequencies, in contrast to the NC. With the normalized frequency $\Omega=\omega/(\gamma 4\pi M)$, the ellipticity is given by

$$R=\frac{2\Omega}{1+\sqrt{1+4\Omega^2}}. \tag{11}$$

For the present samples, for 69 GHz, $\Omega\sim 1$ and $R\sim 0.62$. In the case of 17 GHz, $R\sim 0.24$, and for 9 GHz, $R\sim 0.13$. It should be noted that these values hold only for the main mode. For high-order modes, H_n and, consequently, the ellipticity are lower. Due to $R=R(\Omega)$, also $K_s^{\rm eff}=K_s^{\rm eff}(\omega)$.[2] The effect is illustrated easily by the limiting cases. For $\omega/\gamma \ll 4\pi M$, one finds $K_s^{\rm eff}\to 0$, whereas $K_s^{\rm eff}\to -K_s/2$ for $\omega/\gamma \gg 4\pi M$ (however, the latter case is practically impossible for Fe-Co at common frequencies).[23] The frequency and the surface anisotropy therefore strongly influence the mode intensities which, in any case, decrease more rapidly with n than in the NC.

The first feature we discuss for the PC measurements concerns the main mode. Figure 5 shows a film with $d=1200$ Å . The finding of apparently one broad line, in some cases with a shoulder on the low-field side, is common for all our films above $\sim$ 1000 Å . However, broadening effects are not sufficient as an explanation. The main point is that the lower-order lines are overlapping. We show that the broad feature around 15 kG can be decomposed into three lines.

The spectra displayed in Fig. 5 were measured with the film placed at different positions in the waveguide. This leads to different ''degrees of antisymmetric excitation;'' i.e., the symmetry of the exciting high-frequency field with respect to the center of the film is varied. As the first and third modes couple to symmetric, the second to asymmetric components of the high-frequency field, the relative intensities of these modes are changed. In this way it can be seen that the main feature is, in fact, built up by the first three lines which is shown directly in the theoretical spectrum. In principle, one may fit the spectra using a total microwave absorption given by

$$a\,\mathrm{Re}(Z_s)+b\,\mathrm{Re}(Z_a). \tag{12}$$

$\mathrm{Re}(Z_{s,a})$ stands for the real part of the surface impedance (symmetric and antisymmetric contributions, respectively) which is calculated from the CT.[5] This is not done here as the precise value of the experimental parameter a/b is difficult to adjust.

The second feature concerns the higher-order modes. An example is displayed in the low-field part of Fig. 5. The agreement of the experimental and theoretical line position is excellent (spacing to the main mode better than 2%). Again, we stress that the same parameters also fit the NC spectra. In our simulations, the satellite is identified as the fourth symmetrical mode, i.e., the seventh of all modes.

It is interesting to take a look at the field distance $\delta H_{nn'}$ to the main mode. Using $2A/M=2.87\times 10^{-9}$ G cm^2 from the NC measurements of this film, in a simple $k=n\pi/d$ model $\delta H_{nn'}\sim 7$ kG would correspond rather to $n^2-n'^2=6^2-0=36$ than to $n^2-n'^2=7^2-1^2=48$. In fact, due to the smaller effective K_s in the PC, the surface spins are ''more unpinned,'' and, hence, the main mode has more

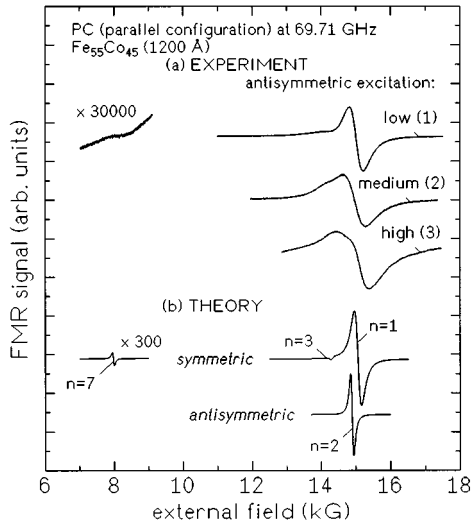

FIG. 5. 69.71 GHz spectra (1200 Å $Fe_{55}Co_{45}$ on glass) in the PC for different excitation conditions. For No. 1 the film was glued onto the waveguide wall at a position of maximum magnetic high-frequency field and vanishing electric field. No. 2 was recorded with the film serving *as* the wall. The microwaves then penetrate only from one side of the film. As this leads to a reasonable excitation of antisymmetric modes (due to high-frequency currents in the film plane), this configuration was also used for most measurements in the NC. For No. 3 the film is placed within the waveguide at a distance of $\sim$ 1 mm from the wall where the electric field is significant, leading to a highly asymmetrical excitation and already a distortion of the line shapes. The theoretical spectrum was calculated using $A=2.6\times 10^{-6}$ erg/cm, $4\pi M=$ 22.75 kG, $K_s=0.5$ erg/cm^2, $g=2.09$, $\rho=8\times 10^{-6}$ Ω cm, and $\lambda=6.5\times 10^7$ rad/s which fit also the NC spectra of this film. As the setup No. 1 has the best signal-to-noise ratio, it is used for the detection of the $n=7$ satellite. The satellite is still on the low-field tail of the main modes and, therefore, the shape is heavily distorted. (In fact, the line position $H_{n=7}$ corresponds to the ''saddle point'' of the signal at 8 kG. The modes between 8 and 14 kG are even more distorted as they are closer to the intense main mode and, therefore, not shown. For the 1500 Å film of Fig. 1, the distortion is even more significant than for the 1200 Å shown here as the lines are closer to each other.) As in the NC, the higher-order modes are broadened by thickness fluctuations. If this is taken into account, there is reasonable agreement with the intensities $[\sim S_p\times(\Delta H)^2]$ given in Table II although the gain factors displayed in the spectra are different.

the character of $n=0$. Consequently, the satellite had to be labeled $n=6$ in this picture. The value of such an argumentation is to find an easy clue to the mode character; however, it is led mainly by plausibility. For unambiguous statements, the more rigorous analysis by CT is necessary which is, moreover, applicable also in cases where $\delta H_{nn'}\sim(n^2-n'^2)$ would yield noninteger values.

This satellite is also used to demonstrate the sensitive dependence of the intensity on K_s which helps to determine this quantity. In Table II, we calculate the ratio of the intensities of the main and the fourth symmetrical mode. The strong dependence on K_s is obvious. $K_s<0$ is not included as the intensity ratio is even more extreme and the higher-order modes are even more difficult to detect in the experiment at the PC.

TABLE II. Calculated intensity ratio of the first and fourth symmetric mode ($n=1$ and 7 of all modes) for $d=1200$ Å in the PC for different frequencies and K_s values and material parameters as displayed in Table I. The experimental value for the intensity ratio at 69.7 GHz is $\sim 2\times 10^{-5}$. At 48.8 GHz, where the line position of the $n=7$ satellite is already close to the zero field, the signal was not sufficient for a reliable intensity determination.

Frequency (GHz)	K_s (erg/cm^2)	Intensity ratio
48.8	1.0	1.2×10^{-4}
	0.5	2.3×10^{-5}
	0.0	1.8×10^{-7}
69.7	1.0	1.7×10^{-4}
	0.5	4.1×10^{-5}
	0.0	3.0×10^{-7}

V. DISCUSSION AND CONCLUSIONS

From our analysis of the experimental data and from additional simulations comparing the results of the CT for the real ρ and an artificially high ρ (insulator) the following can be concluded.

The line *positions* H_n are well described by IT for the material parameters of Fe-Co, $K_s>0$, and $d\sim$ 1200–1500 Å (intermediate thicknesses). For $d\sim\delta$ (some 100 Å) and thick films ($>$ 2000 Å), CT should be used (difference to IT some 10 G and $>$ 100 G, respectively). For $K_s<0$, the deviations of IT from CT are generally large (some 100 G) which is connected particularly with the surface mode in the NC.[16] In the PC, the change of the ellipticity and $K_s^{\rm eff}$ with n is a considerable effect. The most important point for the PC is, however, the decomposition of the main mode structure (see Sec. IV).

It should be noted that the influence of the conductivity on the line position (and other experimental data) is not specific for the Fe-Co alloy system but a general result of the CT. The thickness ranges and the strength of the impact, however, vary for different material parameters.

With respect to the *line width*, it is obvious that CT has to be used when the exchange-conductivity effect can broaden the line by more than 100 G as shown in Fig. 3 for the main mode ($d=1500$ Å). For thin films, however, an analysis based on the insulator approximation as in Ref. 6 is justified. At 48.8 GHz, for the 212-Å film of Fig. 4, the exchange-conductivity broadening amounts to only 2 G.

Because of the finite penetration depth of the exciting high-frequency field, it can already be expected intuitively that the *intensities* cannot be properly described by IT. As in the PC both the ellipticity and the penetration depth of the high-frequency field are a function of n,[5] and the use of CT seems inevitable.

Under certain conditions (low λ and ρ, high A, etc.) the electromagnetic waves and spin waves are strongly mixed as discussed theoretically in Refs. 2,24. Pure Fe was found to be a material with a typical crossover behavior near resonance in the PC for commonly used frequencies. Without going into details of these effects we would like to point out that this also applies to Fe_xCo_{1-x} for x at least down to 0.5 as λ is comparably low and the normalized exchange-conductivity parameter[2,24]

TABLE III. Exchange parameter A for the Fe_xCo_{1-x} system. Besides A, we also give the spin-wave stiffness $D=(2A/M)g\mu_B$ defined via the magnon energy $E=Dk^2$ (Ref. 2). For Co, different structures were stabilized by epitaxy and different preparation conditions.

	A (10^{-6} erg/cm)	D (meV Å^2)	Ref.
Fe (bcc)	2.0	280	2,25
$Fe_{0.55}Co_{0.45}$ (bcc)	2.7	360	this work
Co(bcc)	1.8	330	26
Co(fcc)	1.1–1.3	210–260	2,27
Co(hcp)	2.9	510	25

$$E=\frac{4\pi}{c^2}\frac{\gamma A}{\rho M} \tag{13}$$

can be even higher than for pure Fe ($E=2.79\times 10^{-5}$; for an extensive discussion see Ref. 2).

The apparent similarity of $g(x)$ and $\lambda(x)$ can be qualitatively explained on the basis of the spin-orbit coupling as the relevant interaction.[6,7] A really quantitative analysis depends on a detailed knowledge of the spin-orbit coupling parameter, density of states, and electron scattering frequency as a function of x. In order to obtain a precise theoretical value of λ, most probably also a more sophisticated model would be required.

In Table III, we list the value for A and $D=(2A/M)g\mu_B$ which determines the magnon energy $E=Dk^2$ (for small k) (Ref. 2) together with those for the pure elements. For Co prepared in different structures, an interesting discussion was presented in Ref. 26. The authors found that, surprisingly, the exchange stiffness of Co seems to scale with the near-neighbor coordination which would be expected in a local but not in an itinerant model.

We compare the parameters within the bcc phase. For $Fe_{0.55}Co_{0.45}$, D is significantly larger than for pure Fe (but similar to bcc Co). In contrast, g and λ and, e.g., the magnetization and also the lattice parameter[9] are not very different for $x=0.55$ and 1.

Assuming T_c to scale with D one would expect a smaller difference of $D(x=0.55)$ and $D(x=1)$ than observed because $T_c(x=0.55)/T_c(x=1)=1243$ K/1184 K$=1.05$ (i.e., only at 5% difference), but, of course, it is difficult to understand the value of D in such a simple picture. Here we can only point out some findings which have to be explained by a more elaborated theoretical approach, e.g., electronic structure calculations. A comprehensive analysis of the magnetic properties of the FeCo alloy system and a comparison with theory[8] is in preparation.[28] We note that, for a complete picture, also the possibility to prepare FeCo films in the fcc phase[29] is of high interest.

Finally, in view of the very popular study of K_s in ultrathin films ($d\sim$ 10 Å) using various experimental techniques within the last years,[3] a comment on the different ''methods'' may be useful as SSWR is also a classical technique for the determination of K_s (for $d\sim$ 1000 Å). In each case, the quantity defined in Eq. (3) is evaluated. However, the physical role it is playing in the measurement is not the same, and keeping this in mind is particularly important for

several older SSWR investigations which yielded extremely high K_s values (up to $>$ 10 erg/cm^2).[2]

In general, one may consider (at least) three different situations: first, SSWR on thick films ($\sim$ 1000 Å), yielding $K_s > 1$ erg/cm^2 (in Ref. 2 called ''type I'' films); second, SSWR on thick films with lower K_s (some 0.1 erg/cm^2, ''type II'' films[2]); and third, ultrathin films ($\sim$ 10 Å) with the frequently applied scaling of K_s as an effective volume anisotropy K_s/d,[3] yielding also some 0.1 erg/cm^2 (the values should be taken only as orders of magnitude and may have either sign).

As it is well established that the ''real'' (intrinsic) K_s in most systems is, in fact, some 0.1 erg/cm^2, the question arises how a much higher K_s could be found for some films reported in the literature. The SSWR analysis may indeed yield this K_s value but it should not be considered as the *intrinsic* K_s. The origin of K_s being much higher than 1 erg/cm^2 is most probably in many cases an imperfect structure. An important point is that in usual SSWR analyses the surface anisotropy is treated as an energy located in an infinitely thin volume (the surface) although in reality (particularly in less perfect structures) the interactions (or structural conditions, e.g., dislocations or strain, roughness, etc.) responsible for the effective boundary conditions may be not confined to the very first monolayer. For spin waves with $k^{-1} \sim$ 100 Å and higher, a rather large volume can be felt as the surface contribution to the boundary conditions, i.e., effectively K_s, which is different in experiments on epitaxially grown 10 Å films.

We note that for our (thinner) single-crystalline series on MgO a value in same range as for SSWR on films on glass is obtained from a plot K_s/d over $1/d$ ($K_s \sim$ 0.7 erg/cm^2).

As mentioned in Sec. III, the single-crystalline growth of thick films suitable for SSWR is quite difficult, but, thanks to the ever improving preparation techniques, feasable in some cases (see, e.g., Ref. 27). The investigation of a single-crystalline series of films grown on the same substrate under the very same preparation conditions from about 10 to 1000 Å , i.e., from the regime with $1/d$ scaling to the SSWR region, would be an interesting and also very precise way to determine K_s.

ACKNOWLEDGMENTS

The authors are indebted to V. Drchal, D. Fraitová, J. Kudrnovský, and A. Shick (Prague) for discussions of theoretical aspects. They would also like to thank J. Heise for preparing the samples as well as J. Pelzl, J. Pflaum, and H. Zabel (Bochum) for support in various ways. F.S. acknowledges the hospitality of the Academy of Sciences during his stay in Prague. Financial support from the Grant Agency of the Czech Republic (Project No. 202/95/0015) and the Deutsche Forschungsgemeinschaft (Grand No. SFB 166) is acknowledged.

*Present address: Princeton Materials Institute, Princeton University, Princeton, NJ 08544.

[1] *High Frequency Processes in Magnetic Materials*, edited by G. Srinivasan and A. N. Slavin (World Scientific, River Edge, NJ, 1994); P. E. Wigen, Thin Solid Films **114**, 135 (1984); C. E. Patton, Phys. Rep. **103**, 251 (1984).

[2] Z. Frait and D. Fraitová, in *Spin Waves and Magnetic Excitations*, edited by A. S. Borovik-Romanov and S. K. Sinha (North-Holland, Amsterdam, 1988), and references therein.

[3] B. Heinrich, in *Ultrathin Magnetic Structures*, edited by B. Heinrich and J. A. C. Bland (Springer, Berlin, 1994), Vol. II; B. Heinrich and J. F. Cochran, Adv. Phys. **42**, 523 (1993).

[4] J. O. Artman, Phys. Rev. **105**, 74 (1957).

[5] Ngoc Chan and D. Fraitová, Phys. Status Solidi B **195**, 251 (1996); D. Fraitová (private communication).

[6] F. Schreiber, J. Pflaum, Z. Frait, Th. Mühge, and J. Pelzl, Solid State Commun. **93**, 965 (1995); in that paper, the damping was described by the Gilbert form which is known to be essentially equivalent to the Landau-Lifshitz formalism (Ref. 2).

[7] V. Kamberský, Can. J. Phys. **48**, 2906 (1970); V. Kamberský and C. E. Patton, Phys. Rev. B **11**, 2668 (1975).

[8] I. Turek, J. Kudrnovský, V. Drchal, and P. Weinberger, Phys. Rev. B **49**, 3352 (1994); A. Shick, V. Drchal, and J. Kudrnovský (private communication); M. Battocletti and H. Ebert (unpublished).

[9] *Numerical Data and Functional Relationships in Science and Technology*, edited by K.-H. Hellwege, Landolt-Börnstein, New Series, Group III, Vol. 19, Pt. a (Springer, New York, 1986).

[10] P. Pincus, Phys. Rev. **118**, 658 (1960).

[11] C. H. Wilts and O. G. Ramer, J. Appl. Phys. **47**, 1151 (1976).

[12] R. F. Soohoo, *Magnetic Thin Films* (Harper and Row, New York, 1965).

[13] R. Watts and J. S. S. Whiting, Phys. Rev. B **52**, 457 (1995).

[14] G. T. Rado and J. R. Weertman, J. Phys. Chem. Solids **11**, 315 (1959).

[15] Th. Mühge, Th. Zeidler, Q. Wang, Ch. Morawe, N. Metoki, and H. Zabel, J. Appl. Phys. **77**, 1055 (1995).

[16] Z. Frait, D. Fraitová, C. Dufour, Ph. Mangin, and G. Marchal, IEEE Trans. Magn. **MAG-30**, 711 (1994); and (unpublished).

[17] F. Schreiber, Z. Frait, Th. Zeidler, N. Metoki, W. Donner, H. Zabel, and J. Pelzl, Phys. Rev. B **51**, 2920 (1995).

[18] G. Suran and R. J. Gambino, J. Appl. Phys. **50**, 7671 (1979).

[19] F. Hoffmann, Solid State Commun. **9**, 295 (1971); M. Sparks, *ibid.* **8**, 659 (1970).

[20] G. C. Bailey and C. Vittoria, Phys. Rev. Lett. **28**, 100 (1972).

[21] J. C. S. Levy, Phys. Rev. B **25**, 2893 (1982), and references therein.

[22] As our single-crystalline films are typically $\sim$ 200 Å thick, their linewidths can be analyzed in the insulator approximation using $\Delta H(\omega) = \Delta H(0) + C\omega$ where C is proportional to the intrinsic damping (see Ref. 6 for details). For the Fe-rich side, the inhomogeneity parameter $\Delta H(0)$ is of the order of 10 G; the linewidth, e.g., for the main mode displayed in Fig. 4 at 48.80 GHz, amounts to 60 G.

[23] The usefulness of SSWR measurements in the PC was pointed out by P. Wolf [Z. Angew. Phys. **14**, 212 (1962)] for the limit $K_s^{\text{eff}} \to 0$. However, we remark that the assumption concerning the validity of his Eq. (5) is apparently not fulfilled for the given parameters, so that simple approximations should be taken with care.

[24] D. Fraitová, Phys. Status Solidi B **155**, 281 (1989).

[25] *Ferromagnetic Materials*, edited by E. P. Wohlfarth (North-Holland, Amsterdam, 1980).

[26] J. M. Karanikas, R. Sooryakumar, G. A. Prinz, and B. T. Jonker,

J. Appl. Phys. **69**, 6120 (1991). In this reference the value for D is given (note that the definition differs by the factor $g\mu_B$). For the calculation of A we used $M = 1400$ emu/cm^3 which is close to the theoretical value for bcc-Co. The experimental M value may have been altered by migration of As from the GaAs substrate (see discussion by Karanikas *et al.*); X. Liu, M. M. Steiner, R. Sooryakumar, G. A. Prinz, R. F. C. Farrow, and G. Harp, Phys. Rev. B **53**, 12 166 (1996).

[27] J. A. Wolf, J. J. Krebs, and G. A. Prinz, Appl. Phys. Lett. **65**, 1057 (1994). In this reference also different magnetization values for fcc-Co from the literature are quoted. For the calculation of D one may use a mean value of $M \approx 1300$ emu/cm^3. If a scatter of $\pm$ 200 emu/cm^3 for M is taken into account, the scatter of D is correspondingly higher.

[28] J. Pflaum, F. Schreiber, Z. Frait, J. Heise, Th. Mühge, H. Zabel, and J. Pelzl (unpublished).

[29] M. Zharnikov, A. Dittschar, W. Kuch, K. Meinel, C. M. Schneider, and J. Kirschner, Thin Solid Films **275**, 262 (1996).